Materials Today Bio 31 (2025) 101548

Contents lists available at ScienceDirect

Materials Today Bio

journal homepage: www.journals.elsevier.com/materials-today-bio

A one-two punch of inflammation and oxidative stress promotes revascularization for diabetic foot ulcers

Li Chen [a,1], Yunrong Li [b,1], Xuanxuan Zhang [a,1], Lixin Ma [a,**], Cheng Zhang [a,***], Huanhuan Chen [a,*]

[a] State Key Laboratory of Biocatalysis and Enzyme Engineering, Hubei Key Laboratory of Industrial Biotechnology, School of Life Sciences, Hubei University, Wuhan, 430062, PR China

[b] Guangxi International Zhuang Medicine Hospital Affiliated to Guangxi University of Chinese Medicine, Guangxi, 530201, PR China

ARTICLE INFO

Keywords:
Engineered living materials
Nitric oxide
Wound healing
Angiogenesis
Anti-inflammation

ABSTRACT

Patients with diabetic foot ulcers (DFU) suffering from severe lower limb ischemia face the risk of amputation. Concomitant oxidative stress and hyperinflammation commonly manifest within the tissue affected by DFU, exacerbating the deterioration of DFU wounds. One-two punch strategy of anti-oxidative damage plus anti-inflammatory is anticipated to tackle the challenge of non-healing diabetic wounds. Here, we introduced a dual-approach treatment strategy involving the probiotic *Weissella cibaria* (WC) modified with desferrioxamine (DFO). This engineered probiotic, known as WC@DPA, aims to ameliorate oxidative stress within the ischemic microenvironment and stimulate the formation and proliferation of endothelial tubular structures. When applied with chronic wounds and ischemic hindlimb injuries in diabetic mice, WC@DPA gel demonstrated an effective performance in modulating oxidative damage, reducing local vascular inflammation, and facilitating muscle tissue repair and vascular reconstruction. We believe that our engineered probiotic represents a promising therapeutic avenue for managing ischemic injuries associated with DFU.

1. Introduction

Diabetic foot ulcers (DFU) are a widespread and critical complication among diabetic patients, affecting an estimated 18.6 million people worldwide [1,2]. Alarmingly, approximately 85 % of those with DFU are at risk of undergoing amputation [3–5]. The amputation rate in DFU is significantly higher, ranging between 10 and 20 times more than in non-diabetic individuals, largely due to severe limb ischemia, which is a predominant cause of lower-extremity amputations [6–8]. Researchers have demonstrated that high glucose levels in diabetic ischemic limbs catalyze the production of an abundance of toxic free radicals. These free radicals significantly inhibit the activity of hypoxia-inducible factors, thereby hindering transcription-mediated tissue repair, cell growth, and proliferation [9–12]. Considering the oxidative imbalance and vascular dysfunction characteristic of the microenvironment in DFU, employing a holistic therapeutic strategy that targets the eradication of toxic free radicals and fosters vascular regeneration may prove beneficial.

However, the effectiveness of current vascular reconstruction techniques in fully restoring blood circulation in limbs affected by ischemic foot ulcers often falls short [13,14]. For instance, while surgical bypass can be effective, it is known to cause extensive trauma, necessitate long recovery durations, and is linked to heightened risks of infections and thrombosis. On the other hand, angioplasty, considered a less invasive option, typically displays lower efficacy [15–17]. Despite their effectiveness in specific severe limb ischemia cases, these procedures do not universally apply to all patients. Therefore, localized revascularization emerges as a critical need, highlighting the urgent demand for innovative solutions in this domain.

Probiotic-based therapies have gained notable recognition in clinical research, especially with the utilization of engineered bacteria for wound healing, as evidenced by a growing volume of studies [18–20]. *Weissella cibaria* (WC), a probiotic used in oral healthcare, has been recognized for its anti-inflammatory and antibacterial properties [21,22]. Research indicates that WC can synthesize nitric oxide (NO) locally,

* Corresponding author.
** Corresponding author.
*** Corresponding author.
E-mail addresses: malixing@hubu.edu.cn (L. Ma), zhangcheng1988@whu.edu.cn (C. Zhang), chenhh1008@163.com (H. Chen).
[1] L.C., Y.L. and X.Z. contributed equally to this work.

https://doi.org/10.1016/j.mtbio.2025.101548
Received 12 June 2024; Received in revised form 5 December 2024; Accepted 3 February 2025
Available online 4 February 2025

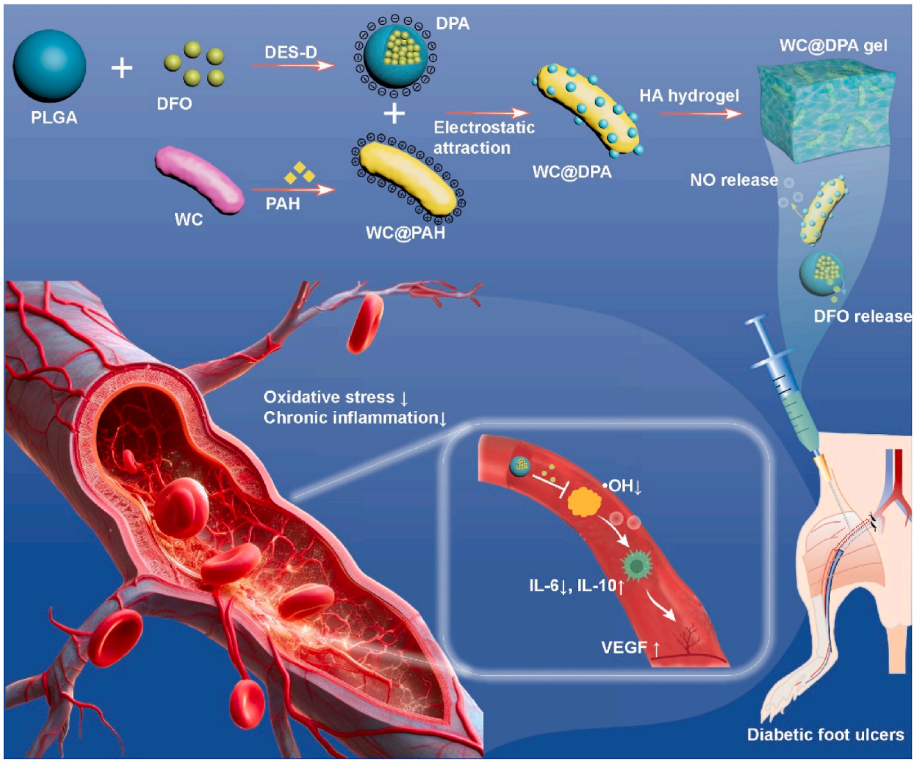

Scheme 1. Schematic illustration of engineered probiotic WC@DPA gel promoted revascularization after limb ischemia injury in DFU. The WC@DPA gel is capable of releasing NO and DFO into the ischemic regions to relieve oxidative stress and chronic inflammation.

aiding in regulating cardiovascular functions and stimulating the activation of skin cells, thereby facilitating angiogenesis [23]. However, the efficacy of WC alone in treating ischemic limbs in diabetes falls short of ideal standards, primarily due to the high glucose levels in diabetic ischemic limbs, which catalyze the production of an abundance of toxic free radicals. Deferoxamine (DFO), a Food and Drug Administration (FDA) approved iron chelator, has been shown to mitigate the production of free radicals, contributing to wound healing and reducing tissue necrosis in DFU [24–27].

Here, we have developed an engineered probiotic hydrogel aimed at overcoming the complex challenges imposed by limb ischemia in DFU. This innovative remedy is accomplished through the strategic union of DFO liposomes and WC, catalyzing a symbiotic relationship (WC@DPA) to mitigate oxidative stress and hyperinflammation, ultimately facilitating vascular reconstruction in DFU (Scheme 1). This WC@DPA was then integrated into a hyaluronate gel, resulting in a potent and therapeutic engineered probiotic gel (Scheme 1). The WC@DPA gel possesses unique qualities, such as nullifying detrimental hydroxyl free radicals, rebalancing oxidative states, and reshaping the chronic inflammatory landscape of DFU. In addition, WC inherently maintains a continual production of NO facilitating localized delivery to the ischemic regions, which is particularly beneficial for enhancing blood circulation in the lower limbs. Our empirical evidence strongly indicated that the dual action of DFO liposomes and the NO-releasing engineered WC markedly improved cell survival, migration, and oxidative stress management, and expedited the re-establishment of angiogenesis and muscle regeneration.

1.1. Materials and reagents

Poly(allylamine hydrochloride) (PAH; Mw: 17 500 Da), Hyaluronic acid (HA), poly (lactic-co-glycolic acid) (PLGA), and 4′,6-diamidino-2-phenylindole (DAPI) were purchased from Sigma-Aldrich (USA). WC was obtained from the BNCC Research Center for Engineering Technology of microbial strains (Henan, China). 2′,7′-dichlorofluorescin diacetate (DCFH-DA), live & dead viability assay kit, and total nitric oxide assay kit were obtained from Beyotime Institute of Biotechnology (China). Hydroxyl free radical scavenging capacity assay kit was purchased from Sangon Biotechnology (China). The mouse IL-6/IL-10 ELISA kit was obtained from Elabscience Biotechnology (China).

1.2. Preparation and characterization of DPA

DPA liposomes were prepared using the double emulsion solvent diffusion (DES-D) method. Initially, DFO (20 mg) was dissolved in 1 mL of 2.8 % Polyvinyl alcohol (PVA)solution and then emulsified with 3 mL of ethyl acetate containing 3 % PLGA [26]. This mixture was sonicated using a probe sonicator at 25 % amplitude for 120 s to create the primary emulsion. The emulsion was then transferred into 10 mL of a 20 % sucrose solution, followed by a secondary sonication for 120 s. Subsequently, the mixture was stirred at room temperature overnight to facilitate the complete evaporation of the ethyl acetate. The DFO liposomes were then collected by centrifugation at 9000 g for 10 min and washed three times with deionized water.

1.3. Synthesis of WC@DPA hydrogel

WC was initially modified with a positive charge via the addition of PAH to get the positively-charged WC. Next, 1 mL of PAH-modified WC solution was blended with 2 mg of DPA (1 mg/mL) in ultrapure water and gently shaken for 60 s. The resulting solution was centrifuged at 6000g for 3 min to obtain the engineered probiotic WC@DPA. The WC@DPA, following formulation, was composed of 1×10^8 CFU/mL WC, 2 μM DFO. The preparation of hyaluronic acid hydrogel was carried out according to the literature [28]. To prepare the HA hydrogel, 2.0 g of HA was dissolved in 100 mL of deionized water, followed by the addition of 6 mL of MA. The pH was adjusted to 7.25, and esterification was performed at 4 °C for 24 h. The resulting mixture was precipitated with

75 % ethanol, dialyzed, and freeze-dried. Next, 1 % 2-methylpropanone and 10 % HA hydrogel were added to a WC@DPA (10^8 CFU/mL) MRS medium solution, which was then exposed to 405 nm blue light for 15 s. Finally, the mixture was left at room temperature to get the WC@DPA gel.

1.4. Swelling rate

After lyophilizing the prepared HA hydrogel, it was immersed in PBS and periodically removed at 37 °C. The surface water was removed using filter paper, and the hydrogel was then weighed. The swelling ratio of the hydrogel was calculated using the following formula:

$$\text{Swelling Ratio (\%)} = (W_b - W_a) / W_a \times 100\%$$

where W_a and W_b represent the weights of the hydrogel before and after immersion in PBS, respectively. The swelling rate experiment of WC@DPA was conducted in the same manner as for the HA hydrogel. Each sample was tested in triplicate.

1.5. Rheology

The storage modulus (G') and loss factor (G″) of WC@DPA hydrogel were evaluated using an HR 20 rheometer. A strain scan test was conducted at 37 °C with a constant frequency of 1 %, ranging from 1 to 100 rad/s.

1.6. NO detection

NO-sensitive fluorescence probe DAR-1 (20 μM) was added to the WC cultures which was then incubated in MRS medium with shaking culture at 37 °C [29]. NO fluorescence intensity (excitation at 566 nm, emission at 586 nm) was measured using a microplate reader. Furtherly, the Griess assay was used to examine the NO concentration of WC.

1.7. •OH detection

Aliquots of DFO at various concentrations were prepared in 10 mL volumetric flasks, with a corresponding volume of distilled water serving as a control for blank measurements. Initially, 1 mL of o-phenanthroline (5 mM) was added, followed by 4 mL of a pH 7.4 phosphate buffer solution and 1 mL of 5 mM $FeSO_4$ solution. The volume was then brought to 10 mL with methanol. At 20 min intervals, the absorbance of the superoxide anion radical system was monitored using a UV spectrophotometer at a wavelength of 320 nm [30].

1.8. Intracellular ROS detection

RAW264.7 cells were seeded at a density of 5×10^4 cells per well in the lower chamber of a 24-well transwell system. The control group was cultured in basal 1640 medium, while the experimental groups were incubated with 100 μM H_2O_2 for 1 h. Following this oxidative challenge, the H_2O_2 group was cultured in basal 1640 medium at 37 °C, while the WC@DPA gel group received WC@DPA gel in the upper chamber of the 24-well transwell, also maintained at 37 °C. After 24 h, all cell groups, now incubated with DCFH-DA fluorescent probes in darkness at room temperature for 30 min, were imaged using a confocal laser scanning microscope (FV1000, Olympus, Japan).

1.9. Anti-inflammatory effect of WC@DPA gel in vitro

To evaluate the anti-inflammatory effect of WC@DPA gel on RAW264.7 cells treated with LPS, we placed RAW264.7 cells at a density of 5×10^4 cells per well in the lower chamber of a 24-well transwell plate. WC@DPA, DPA of WC gel was added to the upper chamber. After incubation, the cells were stained with F4/80 (Biolegend, 123109), CD86 (Biolegend, 159203), and CD206 (Biolegend, 141707) antibodies and imaged using confocal laser scanning microscopy.

1.10. Cell proliferation

HSFs were cultured in a medium containing 33 mM glucose (5×10^4/well) and exposed to 1 % O_2 for 6 h. WC@DPA, DPA or WC gel was respectively added to the upper chamber. The viability of HSFs was assessed using Calcein-AM staining, followed by confocal laser scanning microscopy. Quantitative analysis of the results was performed using ImageJ software.

1.11. Tube formation assay

Human umbilical vein endothelial cells (HUVECs) were seeded into a Matrigel-coated lower chamber, in a medium with 33 mM glucose (5×10^4/well) under 1 % O_2 for 6 h [31]. The tube formation was visualized and imaged using an optical microscope.

1.12. Transwell migration assay

HUVECs were seeded into a Matrigel-coated upper chamber at a density of 1×10^4 cells per well as per protocol [32]. The lower chamber was supplemented with either DPA, WC or WC@DPA gel. HUVECs that had migrated to the bottom surface were stained with a 0.5 % crystal violet solution for 1 h, and then imaged and quantified using an optical microscope.

1.13. Scratch wound healing assay

HUVECs were subcultured in the lower chamber at a density of 1×10^5 cells per well. A sterile p200 pipette tip was used to create a scratch, followed by washing with PBS to remove detached cells [33].

1.14. Evaluations of diabetic wound healing model

The animal experiments were conducted with Balb/C male mice (about 25 g in weight), following our previously established protocol. Briefly, the diabetic mice were injected intraperitoneally with 100 mg/kg streptozotocin (STZ) daily for two consecutive days [34]. Animal experiments were conducted in accordance with the ethical guidelines of the Animal Ethics Committee of Hubei University. The mice were randomly divided into five groups: the acute wound group (Non-DM), the diabetic chronic wound group (DM-Control), the DPA gel group (DM- DPA), the WC gel group (DM-WC), and the WC@DPA gel group (DM-WC@DPA). All mice were housed under a 12 h light/dark cycle. Wound healing progress was monitored by photographing the wounds every other day, and these images were analyzed using ImageJ software. After 14 days of treatments, all mice were sacrificed and collected skin tissues for evaluation, including hematoxylin and eosin (H&E) staining, Masson's trichrome staining, enzyme-linked immunosorbent assay with IL-6 and IL-10, immunohistochemistry/immunofluorescence staining for CD31/DCFH-DA [35].

1.15. Hindlimb ischemia model in diabetic mice

In the establishment of a limb ischemia model, diabetic mice underwent surgery on the left hindlimb. One left hind limb of each mouse was ligated with 7.0 silk thread at the distal ends of the femoral artery and vein, respectively, and ligated at the suture to create a lower limb ischemia model [36–39]. Post-ligation, the skin incision was sutured, and the implicated hydrogels were implanted at the site. The real-time blood flow in both hindlimbs was detected using moorFLPI imaging systems (Moor instruments, UK) every two days [40]. After 14 days of treatments, all mice were sacrificed and collected limb tissues for evaluation, including hematoxylin and eosin (H&E) staining, Giemsa

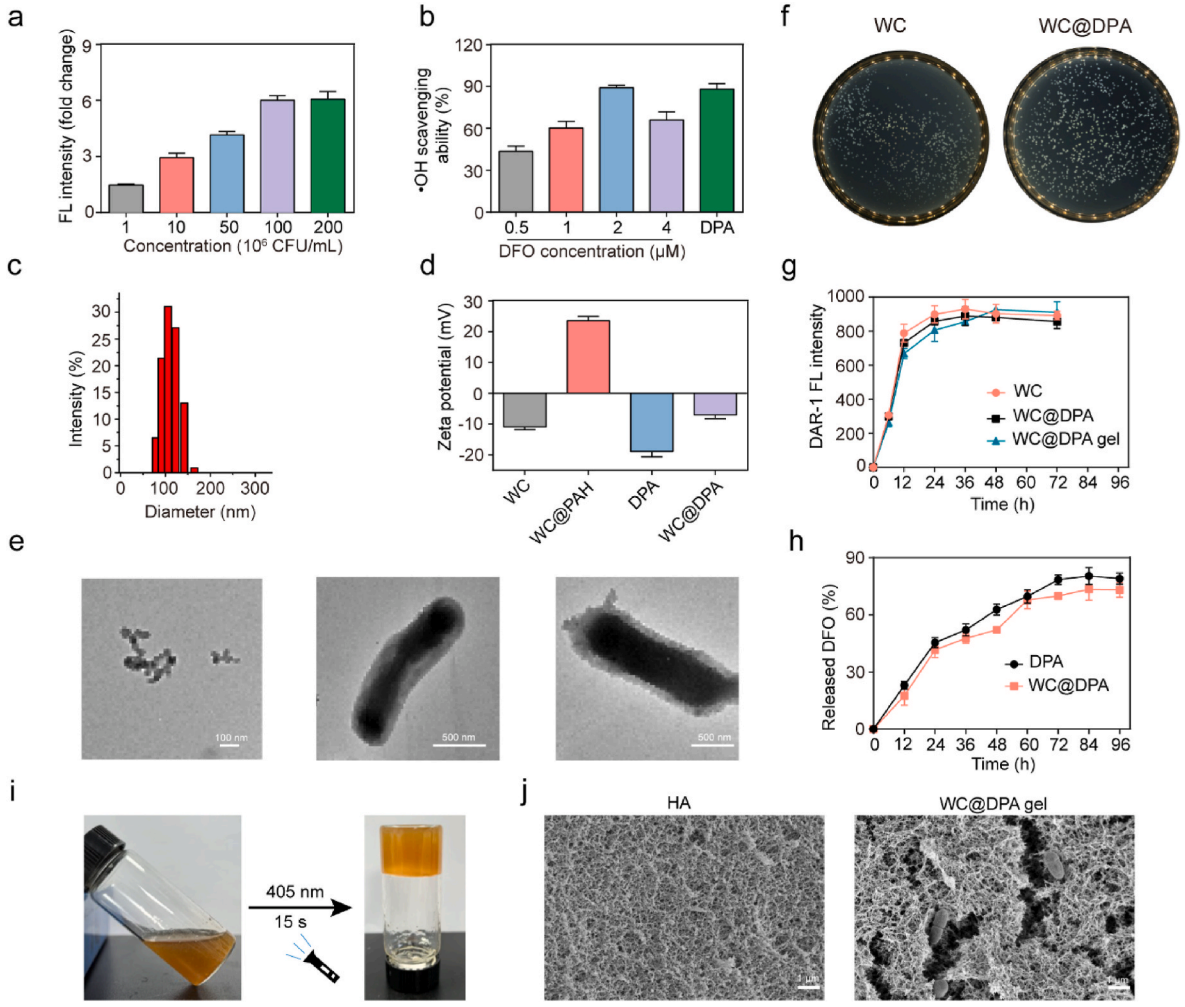

Fig. 1. Characterization of WC@DPA gel. (a) The fluorescence (FL) intensity of the NO-specific probe DAR-1 from different concentrations of WC. (b) The scavenging effect of •OH from different concentrations of DFO and DPA. (c) The hydrated diameter of the DPA liposomes. (d) Zeta potential changes during the preparation of WC@DPA. (e) Representative TEM images of the WC, DPA and WC@DPA. (f) Images of the bacterial colonies of WC and WC@DPA. (g) The fluorescence (FL) intensity of the NO-specific probe DAR-1 among WC, DPA and WC@DPA. (h) DFO release curves between DPA and WC@DPA. (i) Observation of WC@DPA hydrogel formation by inverting the glass tube. (j) Representative SEM images of the HA and WC@DPA hydrogels.

staining, polymerase chain reaction (PCR) array, immunofluorescence staining for dystrophin, CD31 and vascular endothelial growth factor (VEGF).

1.16. Safety evaluation

On day 14, mouse blood is collected for routine hematological and hematology monitoring. The complete blood count (CBC) includes measurements of white blood cells (WBCs), red blood cells (RBCs), and platelets (PLTs). Serum biochemical parameters such as alanine transaminase (ALT) and aspartate transaminase (AST) are also assessed. For histopathological analysis: the major organs of the mice (heart, liver, spleen, lung, kidney) are collected and fixed in 4 % paraformaldehyde (PFA) before undergoing hematoxylin and eosin (H&E) staining.

1.17. Statistical analysis

The data are presented as individual measurements, with bars representing group means ± s.d. Statistical significance was assessed by one-way ANOVA. $p < 0.05$ was considered statistically significant.

2. Results and discussion

2.1. Fabrication and characterization of WC@DPA

In our preliminary investigation, we conducted a preliminary study to assess NO production by live WC, employing the DAR-1 fluorescent probe (Fig. 1a) [41]. Combined with the results of Griess assay, our data revealed that WC, at a concentration of 1×10^8 CFU/mL, generated the highest amount of NO (Supplementary Fig. 1). Consequently, this optimal concentration was selected for use in subsequent experiments. As illustrated in Fig. 1b, the results confirmed WC's ability to produce NO, consistent with the conclusions of our previous research [23]. Concurrently, our study also validated the free radical scavenging ability of DFO through hydroxyl radical detection assays. DFO displayed substantial reduction in hydroxyl radicals at concentrations up to 4 μM, with the most noteworthy effect occurring at 2 μM DFO (Fig. 1b). It was observed that at concentrations exceeding 4 μM, DFO did not exhibit any marked additive effects on free radical scavenging. Following this, we carefully developed DPA liposomes to propagate the examination of their antioxidative capabilities, discovering no significant differences between DFO and DPA (Fig. 1b). The determined size of WC@DPA at the optimal concentration was established at 122.4 nm (Fig. 1c). To facilitate the binding of DPA onto the WC, we initially modified WC's surface

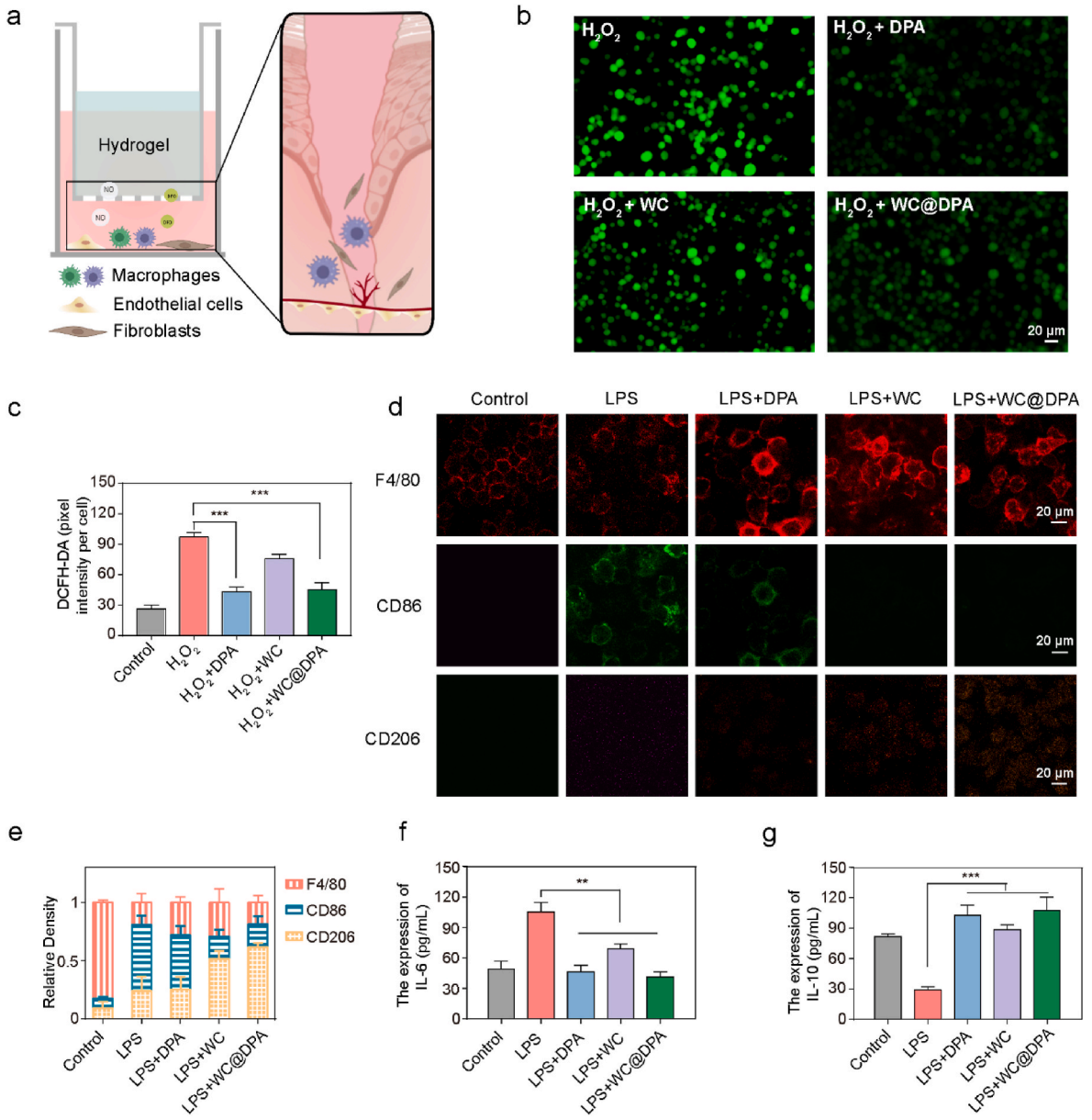

Fig. 2. WC@DPA gel relived inflammation in vitro. (a) Illustration of the wound-healing process treated with WC@DPA gel. Representative images (b) and quantitative analysis (c) of DCFH-DA probe fluorescence intensity in RAW264.7 cells stimulated with H_2O_2. Representative images (d) and relative density (e) of the M1/M2 level in the different groups. The expression level of IL-6 (f) and IL-10 (g) in RAW264.7 cells stimulated by LPS in the different groups ($n = 6$). $^{**}P < 0.01$; $^{***}P < 0.001$.

with biocompatible PAH, conferring a positive charge for subsequent adjustments. Thereafter, the positively charged WC was combined with DPA liposomes to create the biohybrid WC@DPA, exhibiting a zeta of −7.04 mV (Fig. 1d). As shown in Fig. 1e, transmission electron microscopy (TEM) revealed that WC initially had a smooth surface which transformed into a significant granular texture after the incorporation of DPA liposomes. These results confirmed the effective synthesis of DPA with the probiotic.

To verify the growth activity of the probiotic, we incubated both WC and WC@DPA within MRS medium for 24 h. The results demonstrated that the incorporation of liposomes did not impede the growth of the probiotics (Fig. 1f, Supplementary Fig. 2). Moreover, comparative analyses of NO production revealed no significant differences between WC@DPA and its unmodified WC, suggesting that the specific modifications of liposomes did not markedly compromise the functional capabilities of WC (Fig. 1g). To investigate whether the engineered bacteria could facilitated a sustained release of DFO, we introduced probiotics loaded with DFO in PLGA liposomes into a PBS solution. As evident from Fig. 1h, it is clear that an initial 20 % release of DFO within the first 12 h, followed by an approximate 50 % release at 48 h. Subsequent observations pointed to a gradual and consistent drug-release profile beyond the 72 h threshold. The initial quick release phase was likely due to DFO diffusing through the liposome's outer layers, with the prolonged release phase indicative of sustained effusion from the liposome matrix. Furthermore, we used 10 % HA for encapsulation the WC probiotics, capitalizing on its biocompatibility and effective nutrient permeability [28]. Additionally, we characterized the properties of the HA hydrogel. As shown in Fig. 1i, the WC@DPA hydrogel formation was observed by inverting the glass tube. Scanning electron microscopy (SEM) images revealed that HA hydrogel exhibited a typical cross-linked porous structure, while the WC@DPA hydrogel showed bacteria encapsulated within the hydrogel pores (Fig. 1j). Next, we evaluated the

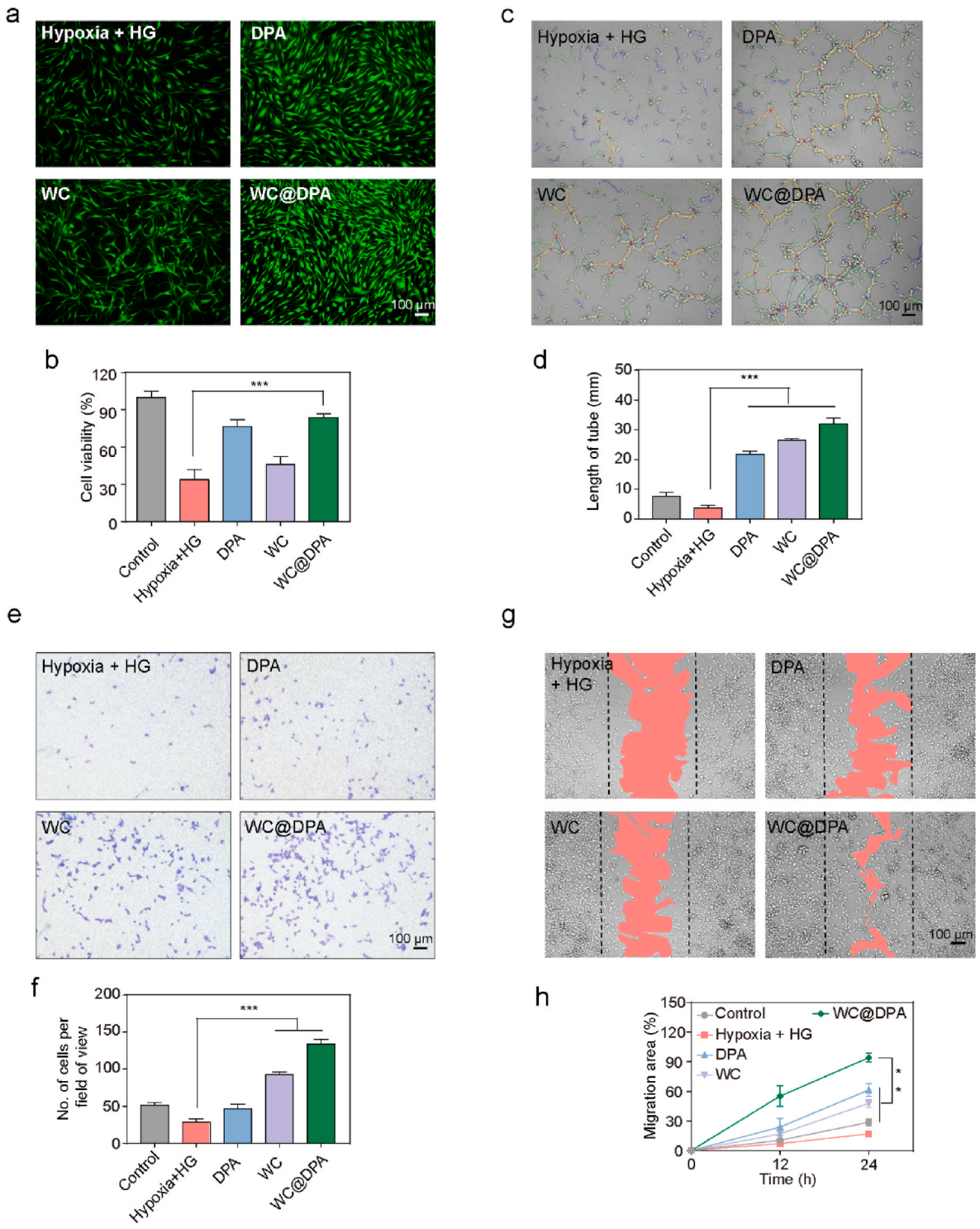

Fig. 3. WC@DPA gel promoted cell proliferation in vitro. Representative images (a) and cell viability (b) of HSFs with 33 mM glucose and 6 h hypoxia in different groups. Representative images (c) and quantitative analysis (d) of tube formation in HUVECs. Scale bar 100 μm. Representative images (e) and quantitative analysis (f) of the transwell migration assay conducted on HUVECs. Representative images (g) and quantitative analysis (h) of migration in HUVECs. $^{**}P < 0.01$; $^{***}P < 0.001$.

swelling behavior of HA and WC@DPA hydrogels. Their weight increased quickly during the initial phase, reaching swelling equilibrium at 12 h, while maintaining gel stability (Supplementary Fig. 3). The viscoelastic properties of the hydrogel were assessed through rheological experiments. To investigate the potential of HA hydrogels as wound dressings, we subjected both HA and WC@DPA hydrogels to a strain sweep ranging from 0.1 % to 1000 %. Within the strain range of 0.1 %–40 %, both hydrogels exhibited elasticity and could return to its original state. However, when the strain exceeded 40 %, both hydrogels began to undergo irreversible deformation (Supplementary Fig. 4). Additionally, the WC@DPA hydrogel demonstrated excellent injectability, making it suitable for subsequent in vivo animal experiments.

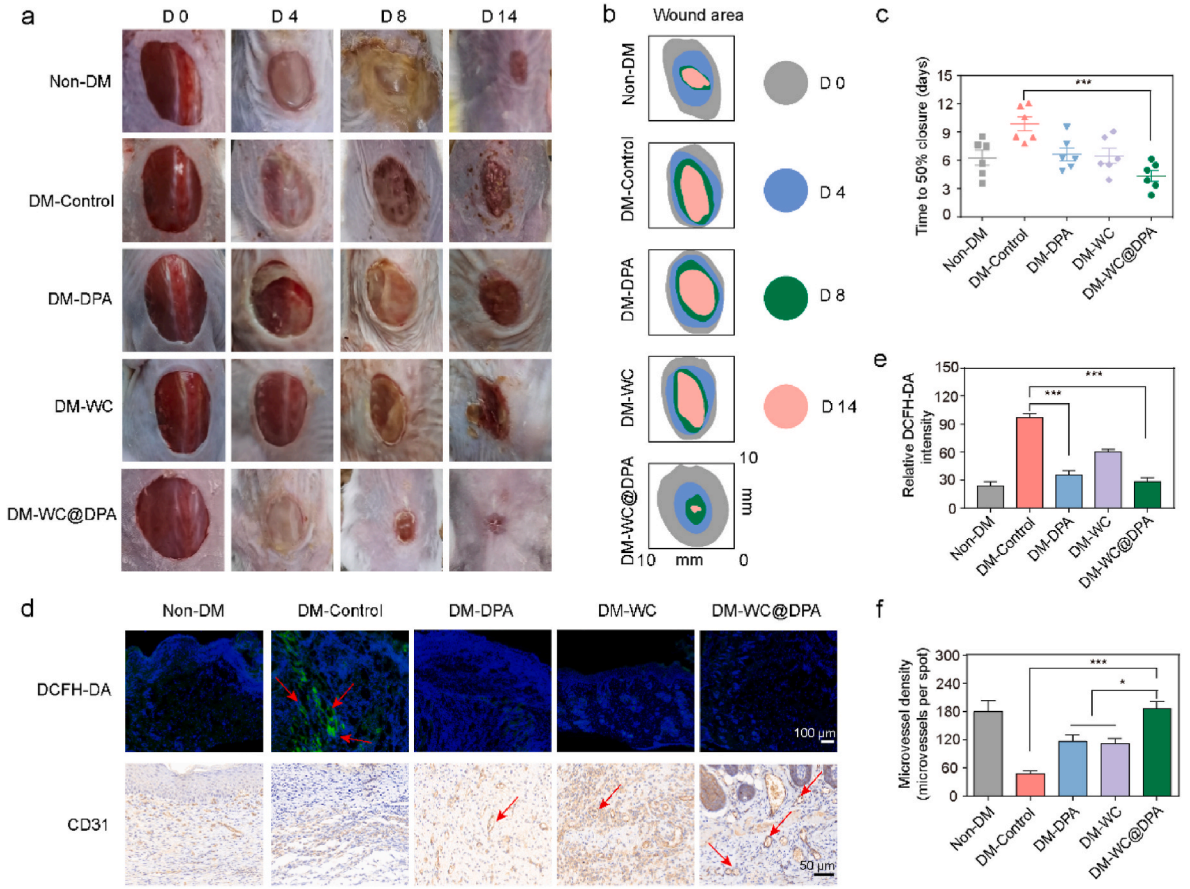

Fig. 4. WC@DPA gel promoted diabetic wound healing. Representative images (a) and closure traces of the wound areas (b) at days 0, 4, 8 and 14 treated with WC@DPA gel or not ($n = 6$). (c) Days of the 50 % wound-closure times ($n = 6$). (d) Immunohistochemical images of DCFH-DA and the blood vessel CD31-positive endothelial cells of wound tissues in different groups. (n = 3). The positive findings were highlighted with a red arrow. (e) Quantitative analysis of DCFH-DA from the wound areas on day 6 in different groups ($n = 3$). (f) Quantitative analysis of the average microvessel densities on day 14 in different groups ($n = 3$). $^{***}P < 0.001$. (For interpretation of the references to colour in this figure legend, the reader is referred to the Web version of this article.)

2.2. WC@DPA inhibited oxidative stress and inflammation

Oxidative stress and chronic inflammation interact to promote the development of DFU [8]. We observed this effect by exposing RAW264.7 macrophages to hydrogen peroxide (H_2O_2) and then co-culturing them with WC@DPA utilizing a transwell system (Fig. 2a) [42]. Our DCFH-DA reactive oxygen species fluorescence staining experiments indicated that WC@DPA gel could alleviate the oxidative stress induced by H_2O_2 (Fig. 2b and c) [43]. Polarization of macrophages to proinflammatory cells (M1-like) or anti-inflammatory (M2-like) phenotype determines the healing process of chronic wounds. Combining our previous research, we found that WC@DPA gel is effective in polarizing M1 macrophages stimulated by lipopolysaccharide (LPS) into M2 macrophages, accompanied by a decrease in CD86 expression and an increase in CD206 expression (Fig. 2d and e). This may be due to the fact that deferoxamine (DFO) is an iron chelator that can reduce iron levels by chelating iron ions, thereby inhibiting M1-type macrophage polarization. On this basis, we also demonstrated that WC@DPA gel can effectively reduce the levels of pro-inflammatory cytokines such as IL-6, and increase the levels of anti-inflammatory cytokine IL-10 (Fig. 2f and g), indicating that NOX gel has anti-inflammatory properties.

2.3. WC@DPA promoted proliferation of skin cells

DFO and NO, released by WC@DPA gel, are posited to interact beneficially with endothelial and skin cells. Previous studies have demonstrated that co-culturing skin cells under high glucose and hypoxia conditions replicates the microenvironment of diabetic foot ulcers [44,45]. We observed a boost in the proliferation of HSFs in both WC@DPA and DPA-treated groups, confirmed by live-dead cell staining assays (Fig. 3a and b). Vascular tube formation by HUVECs cultured on Matrigel was investigated in vitro (Fig. 3c), and co-cultured with WC@DPA was revealed to promote endothelial tube formation, as evidenced by an increasing number of junctional nodes and total tube length (Fig. 3d). Additionally, WC@DPA's positive effects on the migratory abilities of HUVECs were substantiated (Fig. 3e and f), and the scratch assay further confirmed the migration function of WC@DPA on HUVECs (Fig. 3g). Under the dual pressures of high glucose and hypoxia, the scratch wound area was notably smaller when co-cultured with WC@DPA gel, indicating improved wound healing (Fig. 3h). Collectively, these in vitro experiments suggest that WC@DPA not only encourages the formation and growth of endothelial but also contributes to fibroblast proliferation and the migratory response of epidermal cells, thereby promoting wound healing processs.

2.4. WC@DPA accelerates wound healing in diabetic mice

This investigation utilized a chronic diabetic wound model, specifically employing STZ-induced diabetic mice, to examine inflammation regulation and biocompatibility [46]. The STZ-induced mice displayed typical symptoms including weight reduction and decreased blood glucose (Supplementary Fig. 5). Precise full-thickness circular wounds with a diameter of 10 mm were created centrally on the dorsal region of the mice (Supplementary Fig. 6a) [45]. The healing process was

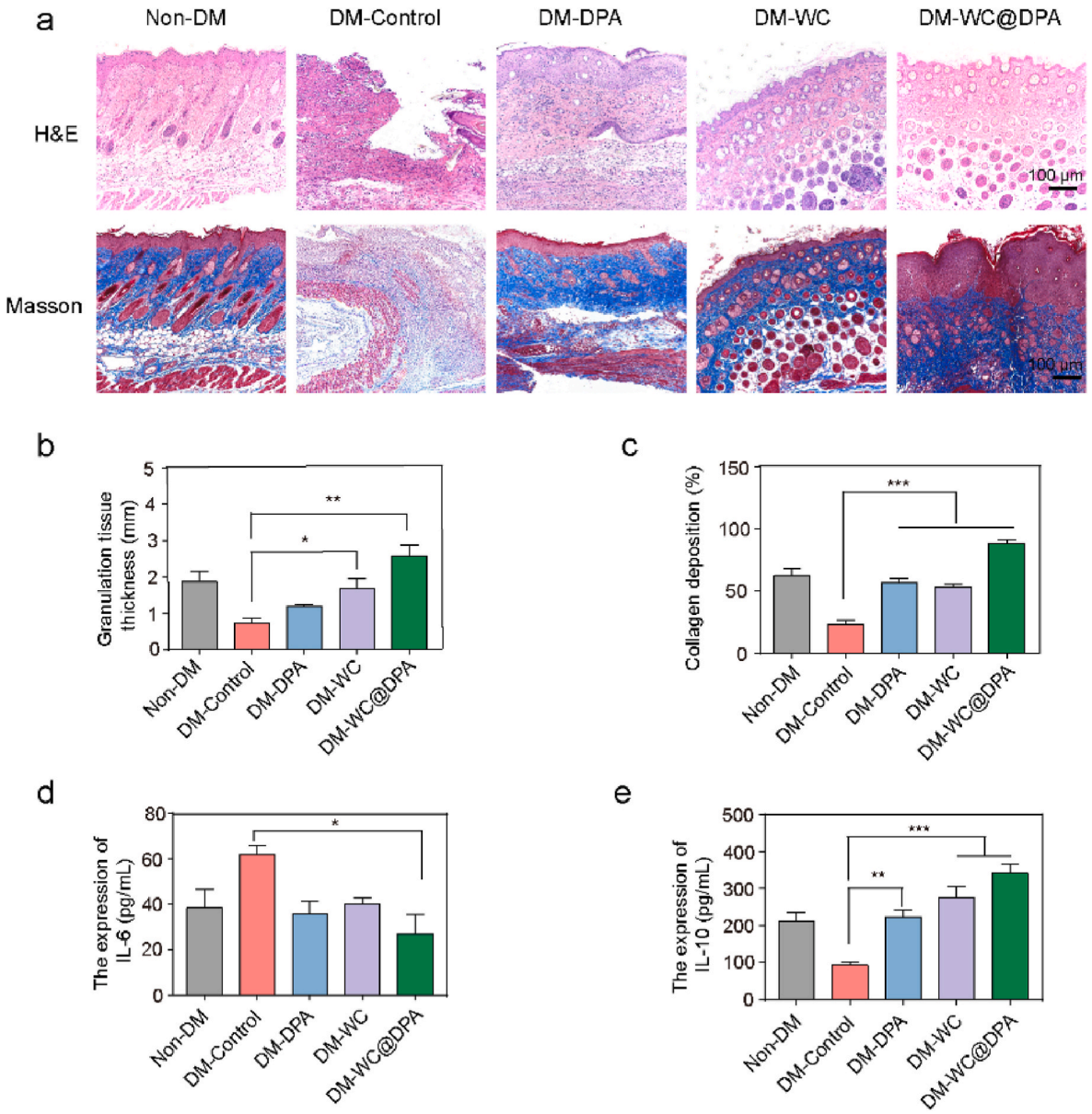

Fig. 5. WC@DPA gel accelerated tissue regeneration. (a) H&E and Masson of wound tissues in different groups at day 14 ($n = 3$). Quantitative analysis of the granulation tissue (b) and collagen deposition (c) in different groups at day 14 ($n = 3$). (d, e) The expression level of IL-6 and IL-10 from wound tissues on day 6 in the different groups. $^{*}P < 0.05$; $^{**}P < 0.01$; $^{***}P < 0.001$.

regularly monitored through photographic documentation, and DPA, WC or WC@DPA gel were routinely administered (Fig. 4a). The healing rates in diabetic mice were markedly slower compared to the Non-DM (non-diabetic) group. However, wounds treated with WC@DPA exhibited the most expedient healing progress (Fig. 4b and c, Supplementary Fig. 6b).

DFO is an iron chelator, which can block the formation of hydroxyl radicals by chelating iron ions, thereby reduce lipid peroxidation damage the level of ROS in cells [47]. ROS levels in skin tissues, assessed on day 6 post-treatment using DCFH-DA staining, were found to be significantly higher in diabetic mice (Fig. 4d). In comparison with Non-DM group, both DPA and WC@DPA treatment effectively reduced ROS levels (Fig. 4e). Moreover, CD31 immunohistochemical analysis revealed enhanced vascular density in WC@DPA-treated mice (Fig. 4d–f).

Further exploration into the therapeutic efficacy of WC@DPA involved the collection of skin samples from each treatment group on day 3, 6 and 14 after treatment for histological analysis (Fig. 5a, Supplementary Figs. 7–8). The DM-Control group exhibited diminished epidermal integrity and a reduction in granulation tissue formation. In contrast, the area treated with WC@DPA gel displayed a more intact epidermis and prolific granulation tissue (Fig. 5b and c, Supplementary Fig. 9). The anti-inflammatory potential of WC@DPA was further investigated by measuring inflammatory mediator levels through ELISA. The DM-Control group had heightened levels of IL-6, which could thwart the wound healing process (Fig. 5d). Treatment with WC@DPA not only diminished the expression of pro-inflammatory chemokine genes like IL-6 but also increased anti-inflammatory IL-10 levels, implicating its efficacy in mitigating inflammation and adverse vascular remodeling (Fig. 5e). These findings indicate that WC@DPA treatment has the potential to alleviate local tissue inflammation and oxidative stress. On day 14 post-surgery, a subset of mice was euthanized for comprehensive organ analysis. Histological examination of major organs, including the heart, liver, spleen, lungs, and kidneys, with H&E staining, confirmed no adverse effects of the engineered probiotics on the mice's normal physiological functions. Sections of major organs showed no residual

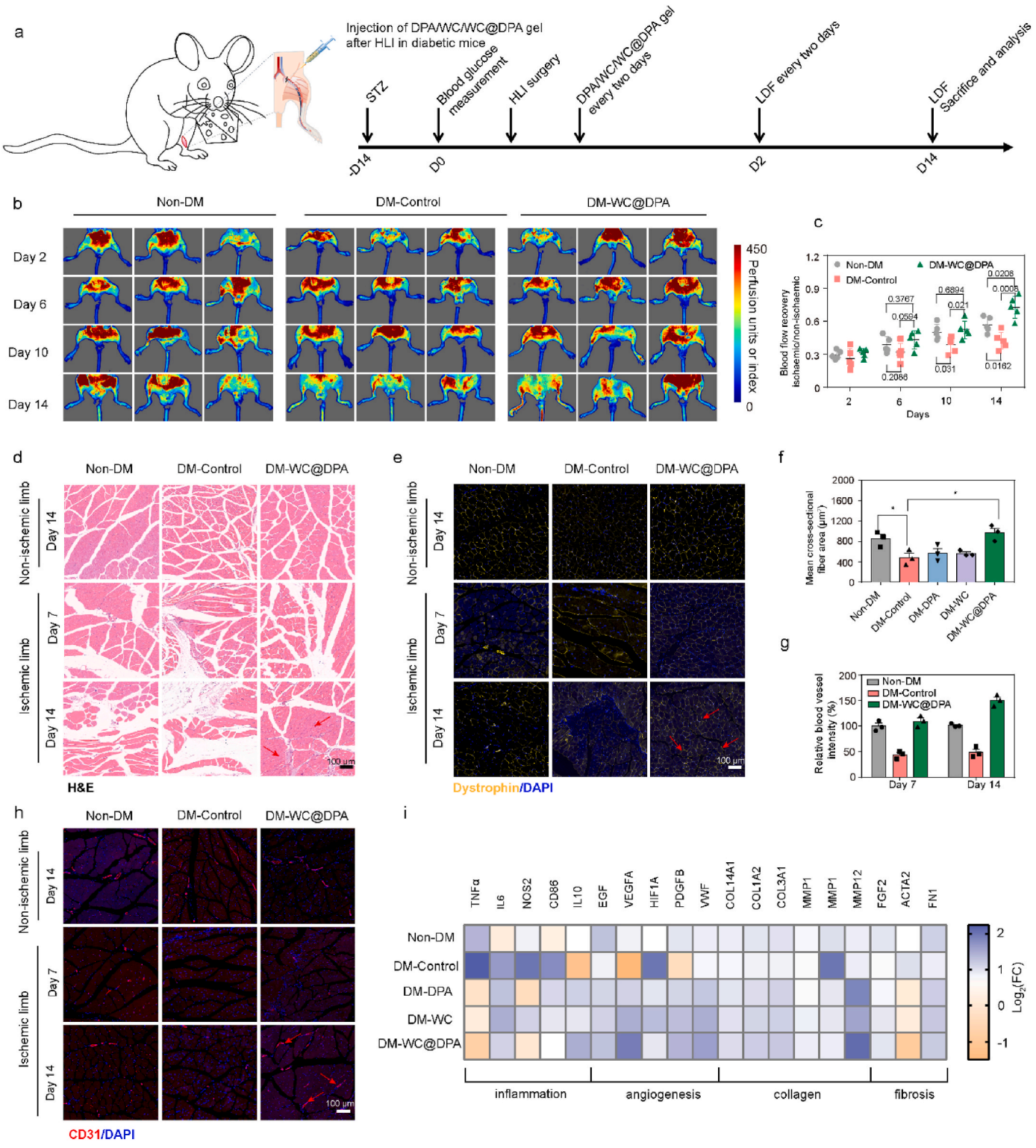

Fig. 6. WC@DPA gel accelerated angiogenesis. (a) Timeline of ischemic limbs treatment process in diabetic mice. (b) Representative laser Doppler perfusion images of the ischemic hindlimbs at days 0, 2, 6, 10 and 14 treated with WC@DPA gel or not. Left leg: non-ischemic; right leg: ischemic. Three technical replicates. (c) Quantitative analysis of blood perfusion as indicated by ischemic/non-ischemic hindlimb ratio. (d) H&E staining of non-ischemic limb and ischemic limb in different groups. Immunofluorescence images (e) and quantitative analysis (f) of dystrophin from non-ischemic limb and ischemic limb in different groups. Immunofluorescence images (g) and quantitative analysis (h) of hindlimbs highlighting blood vessel CD31-positive endothelial cells in different groups. The positive findings were highlighted with a red arrow. (i) Heat map of the fold changes in mRNA expression from ischemic limbs. *$P < 0.05$. (For interpretation of the references to colour in this figure legend, the reader is referred to the Web version of this article.)

bacteria (Supplementary Fig. 10). Furthermore, blood routine examination (WBC, PLT, RBC) and blood biochemical examination of inflammation, liver and kidney function indexes showed that WC@DPA did not induce any significant changes (Supplementary Figs. 11a and b).

2.5. WC@DPA promotes vascular healing in hindlimb ischemia

The adoption of diabetic mice with lower limb ischemic injuries as a model for DFU is a recognized standard that yields essential understanding of the condition's fundamental mechanisms [48,49]. Consistent with existing literature, STZ-treated mice displayed increased lipid core accumulation and lesion formation along the aortic vessel walls [50,51]. To further elucidate the process of vascular healing, we studied the impact of various treatments on muscle repair and vascular remodeling in the ischemic regions of the lower limbs in diabetic mice.

To evaluate the revascularization efficacy of WC@DPA in ischemic injury, we administrated DPA, WC, and WC@DPA to diabetic mice with unilateral hind limb ischemic injury (Fig. 6a, Supplementary Fig. 12). Laser Doppler perfusion imaging indicated a progressive decrease in blood flow within the untreated group, in stark contrast to the WC@DPA treatment group, which exhibited a significant enhancement in blood flow recovery (Fig. 6b and c). H&E staining highlighted severe muscle bundle damage in the DM-Control group, while the WC@DPA-treated mice exhibited a restoration of healthy muscle morphology, unlike the observation in the WC and DPA groups (Fig. 6d, Supplementary Fig. 13). Subsequent staining for anti-muscle atrophy protein underscored WC@DPA gel's significant role in promoting muscle fiber repair, as evidenced by an increased presence of anti-muscle atrophy protein-positive fibers compared to the DPA and WC groups [41] (Fig. 6e and f, Supplementary Fig. 14). Cross-sectional analyses of muscle fibers revealed a reduction in fiber size within ischemic limbs versus non-ischemic limbs across all experimental groups. Notably, the WC@DPA-treated mice demonstrated intact and regular fiber morphology, indicative of a protective or reparative effect relative to the DPA and WC treatment groups. By day 7, the density of CD31-positive capillary in the WC@DPA group was markedly higher than in the DPA and WC groups, thus highlighting the pro-angiogenic effect of WC@DPA (Fig. 6g and h, Supplementary Fig. 15). Our data confirm that applied WC@DPA increases the densities of microvessels, which was consistent with the immunofluorescence of VEGF (Supplementary Fig. 16).

Additionally, Quantitative PCR (q-PCR) assays were employed to evaluate alterations in gene expression during the vascular reconstruction process (Fig. 6i). At 14 days post-surgery, a significant upregulation of pro-inflammatory cytokines (TNFα, IL6, and NOS2) mRNA was observed in the untreated ischemic hindlimbs of diabetic mice compared to their non-ischemic limbs. In contrast, the levels of anti-inflammatory cytokines IL10 and TGFB were substantially reduced in the untreated ischemic limb relative to the treated group. Limbs receiving DPA and WC@DPA treatment demonstrated a pronounced reduction in pro-inflammatory cytokines levels. Regarding genes involved in vascular genesis (EGF, PDGFB, and VWF) and collagen synthesis (COL1A2, COL3A1, COL14A1, MMP1, MMP12) [37,42], these showed negligible expression in non-ischemic hindlimbs, whereas a marked activation was noted in the ischemic limbs of diabetic mice following treatment. Furthermore, expression levels of MMP1, MMP9, and MMP12 were decreased in the WC@DPA-treated group, indicative of advanced collagen fiber maturation. Nonetheless, genes implicated in angiogenesis and collagen development exhibited sustained activity in the WC@DPA group, which suggests ongoing repair and regeneration processes. By performing Giemsa staining on the tissues of the bacterial treatment group, we found no residual bacteria after the treatment was completed (Supplementary Fig. 17).

Despite the widespread application of DFO in diabetic wound healing, unmodified DFO fails to promote vascular reconstruction in diabetic ischemic foot ulcers. As an improvement to DFO, engineered probiotics modified with DFO have been developed for the release of deferoxamine and NO gas to enhance the microenvironment in ischemic lower limbs. This study offers an effective method for angiogenesis and muscle regeneration in diabetic ischemic limbs. Nevertheless, we acknowledge some limitations of this research. Firstly, the STZ-induced diabetic mouse model of hindlimb ischemia we used may not fully mimic the condition in human DFU patients, and the proximal ligation model of the left femoral artery and vein might not achieve severe limb ischemia. To better test the synergistic therapeutic effects of engineered probiotics, future studies could use larger animals, such as pigs, whose pathophysiology is more closely related to humans. Secondly, the dose-response effect of NO release by the engineered probiotics was not studied. High concentrations of NO could pose a risk of NO toxicity. In our future research, we will apply engineered probiotics in a severe ischemia model of the lower limb and study how the treatment duration affects the therapeutic outcomes.

3. Conclusion

In summary, we have successfully developed an innovative engineered probiotic that delivers a synergistic dual action by strategic release of nitric oxide and deferoxamine. These agents work in tandem to modulate hyperinflammation and oxidative stress, thereby promoting angiogenesis in DFU. The therapeutic potential of our WC@DPA gel formulation has been established through meticulous in vitro and in vivo research, which includes its application in diabetic chronic wounds and lower limb ischemia models. Noteworthy, WC@DPA gel demonstrates the ability to accelerate revascularization by day 5 post-treatment, marking a substantial improvement over previous treatment. Additionally, WC@DPA gel significantly reduces the levels of pro-inflammatory cytokines and the presence of deleterious free radicals, thereby transforming persistent low-grade inflammation into a more favorable acute inflammatory response conducive to healing. Reflecting on the stubborn nature of DFU, the application of WC@DPA gel holds great potential for broader therapeutic applications across various wound scenarios, including but not limited to diabetic wounds, burns, scalds, and pressure ulcers.

CRediT authorship contribution statement

Li Chen: Writing – original draft, Formal analysis, Data curation. **Yunrong Li:** Writing – original draft, Methodology, Formal analysis. **Xuanxuan Zhang:** Formal analysis, Data curation, Conceptualization. **Lixin Ma:** Project administration, Conceptualization. **Cheng Zhang:** Writing – review & editing, Supervision. **Huanhuan Chen:** Writing – review & editing, Supervision, Project administration, Conceptualization.

Declaration of competing interest

The authors declare that they have no known competing financial interests or personal relationships that could have appeared to influence the work reported in this paper.

Acknowledgements

This work was supported by the Project of Technological Innovation Plan in Hubei Province (2024BCA001), the Natural Science Foundation of Wuhan City (2024040701010046) and the National Natural Science Foundation of China (32301105).

Appendix A. Supplementary data

Supplementary data to this article can be found online at https://doi.org/10.1016/j.mtbio.2025.101548.

Data availability

Data will be made available on request.

References

[1] International Diabetes Federation, IDF Diabetes Atlas 2021, 10.
[2] D.G. Armstrong, A.J.M. Boulton, S.A. Bus, Diabetic foot ulcers and their recurrence, N. Engl. J. Med. 376 (2017) 2367–2375.
[3] D.G. Armstrong, T.-W. Tan, A.J.M. Boulton, S.A. Bus, Diabetic foot ulcers: a review, JAMA 330 (1) (2023) 62–75.
[4] S.A. Bus, L.A. Lavery, M. Monteiro-Soares, A. Rasmussen, A. Raspovic, I.C.N. Sacco, J.J. van Netten, Guidelines on the prevention of foot ulcers in persons with diabetes (IWGDF 2019 update), Diabetes Metab, Res. Rev. 36 (2020) e3269.
[5] H. Dogruel, M. Aydemir, M.K. Balci, Management of diabetic foot ulcers and the challenging points: an endocrine view, World J. Diabetes 13 (1) (2022) 27–36.
[6] W.J. Jeffcoate, L. Vileikyte, E.J. Boyko, D.G. Armstrong, Current challenges and opportunities in the prevention and management of diabetic foot ulcers, Diabetes Care 41 (4) (2018) 645–652.
[7] P.W. Moxey, P. Gogalniceanu, R.J. Hinchliffe, I.M. Loftus, K.J. Jones, M. M. Thompson, P.J. Holt, Lower extremity amputations-a review of global variability in incidence, Diabet. Med. 28 (10) (2011) 1144–1153.
[8] F. Huang, X.Y. Lu, Y. Yang, Y.S. Yang, Y.Y. Li, L. Kuai, B. Li, H.Q. Dong, J.L. Shi, Microenvironment-based diabetic foot ulcer nanomedicine, Adv. Sci. 10 (2) (2023) e2203308.
[9] I.R. Botusan, V.G. Sunkari, O. Savu, A.I. Catrina, J. Grünler, S. Lindberg, T. Pereira, S. Ylä-Herttuala, L. Poellinger, K. Brismar, S.B. Catrina, Stabilization of HIF-1α is critical to improve wound healing in diabetic mice, Proc. Natl. Acad. Sci. U.S.A. 105 (49) (2008) 19426–19431.
[10] G.L. Semenza, Hypoxia-inducible factors in physiology and medicine, Cell 148 (3) (2012) 399–408.
[11] S.B. Catrina, X. Zheng, Disturbed hypoxic responses as a pathogenic mechanism of diabetic foot ulcers, Diabetes Metabol. Res. Rev. 32 (2016) 179–185.
[12] S.B. Catrina, K. Okamoto, T. Pereira, K. Brismar, L. Poellinger, Hyperglycemia regulates hypoxia-inducible factor-1alpha protein stability and function, Diabetes 53 (12) (2004) 3226–3232.
[13] V. Falanga, R.R. Isseroff, A.M. Soulika, M. Romanelli, D. Margolis, S. Kapp, M. Granick, K. Harding, Chronic wounds, Nat. Rev. Dis. Prim. 8 (1) (2022) 50.
[14] B.R. Freedman, C. Hwang, S. Talbot, B. Hibler, S. Matoori, D.J. Mooney, Breakthrough treatments for accelerated wound healing, Sci. Adv. 9 (20) (2023) eade7007.
[15] F. Benedetto, D. Spinelli, N. Pipito, D. Barilla, F. Stilo, G.D. Caridi, C. Barilla, F. Spinelli, Inframalleolar bypass for chronic limb-threatening ischemia, Vasc. Med. 26 (2) (2021) 187–194.
[16] B. Kim, B.G. Kim, J.K. Seo, G.S. Kim, H.Y. Lee, Y.S. Byun, The predictors of clinical outcome after endovascular intervention for lower extremity peripheral arterial disease, Eur. Heart J. 41 (2020) ehaa946, 2401.
[17] J.A. Beckman, P.A. Schneider, M.S. Conte, Advances in revascularization for peripheral artery disease: revascularization in PAD, Circ. Res. 128 (12) (2021) 1885–1912.
[18] Z. Ming, L. Han, M. Bao, H. Zhu, S. Qiang, S. Xue, W. Liu, Living bacterial hydrogels for accelerated infected wound healing, Adv. Sci. 8 (24) (2021) e2102545.
[19] L. Mei, D. Zhang, H. Shao, Y. Hao, T. Zhang, W. Zheng, Y. Ji, P. Ling, Y. Lu, Q. Zhou, Injectable and self-healing probiotics-loaded hydrogel for promoting superbacteria-infected wound healing, ACS Appl. Mater. Interfaces 14 (18) (2022) 20538–20550.
[20] Z. Xu, X. Yu, F. Gao, M. Zang, L. Huang, W. Liu, J. Xu, S. Yu, T. Wang, H. Sun, J. Liu, Fighting bacteria with bacteria: a biocompatible living hydrogel patch for combating bacterial infections and promoting wound healing, Acta Biomater. 181 (2024) 176–187.
[21] M.S. Kang, D.S. Lee, S.A. Lee, M.S. Kim, S.H. Nam, Effects of probiotic bacterium Weissella cibaria CMU on periodontal health and microbiota: a randomised, double-blind, placebo-controlled trial, BMC Oral Health 20 (1) (2020) 243.
[22] H.J. Jang, M.S. Kang, S.H. Yi, J.Y. Hong, S.P. Hong, Comparative study on the characteristics of Weissella cibaria CMU and probiotic strains for oral care, Molecules 21 (12) (2016) 1752.
[23] H.H. Chen, F.S. Fu, Q.W. Chen, Y. Zhang, X.Z. Zhang, Two-pronged microbe delivery of nitric oxide and oxygen for diabetic wound healing, Nano Lett. 23 (12) (2023) 5595–5602.
[24] C.N. Tchanque-Fossuo, S.E. Dahle, S.R. Buchman, R. Rivkah Isseroff, Deferoxamine: potential novel topical therapeutic for chronic wounds, Br. J. Dermatol. 176 (4) (2017) 1056–1059.
[25] D. Duscher, E. Neofytou, V.W. Wong, Z.N. Maan, R.C. Rennert, M. Inayathullah, M. Januszyk, M. Rodrigues, A.V. Malkovskiy, A.J. Whitmore, G.G. Walmsley, M. G. Galvez, A.J. Whittam, M. Brownlee, J. Rajadas, G.C. Gurtnera, Transdermal deferoxamine prevents pressure-induced diabetic ulcers, Proc. Natl. Acad. Sci. U.S. A. 112 (1) (2015) 94–99.
[26] S.A. El-Gizawy, A. Nouh, S. Saber, A.Y. Kira, Deferoxamine-loaded transfersomes accelerates healing of pressure ulcers in streptozotocin-induced diabetic rats, J. Drug Deliv. Sci. Technol. 58 (2020) 101732.
[27] Z. Ding, Y. Zhang, P. Guo, T. Duan, W. Cheng, Y. Guo, X. Zheng, G. Lu, Q. Lu, D. L. Kaplan, Injectable desferrioxamine-laden silk nanofiber hydrogels for accelerating diabetic wound healing, ACS Biomater. Sci. Eng. 7 (3) (2021) 1147–1158.
[28] Z.Z. Ming, L. Han, M.Y. Bao, H.H. Zhu, S.J. Qiang, S.B. Xue, W.W. Liu, Living bacterial hydrogels for accelerated infected wound healing, Adv. Sci. 8 (24) (2021) 2102545.
[29] Y.C. Sung, P.R. Jin, L.A. Chu, F.F. Hsu, M.R. Wang, C.C. Chang, S.J. Chiou, J.T. Qiu, D.Y. Gao, C.C. Lin, Y.S. Chen, Y.C. Hsu, J. Wang, F.N. Wang, P.L. Yu, A.S. Chiang, A.Y. Wu, J.J. Ko, C.P. Lai, T.T. Lu, Y. Chen, Delivery of nitric oxide with a nanocarrier promotes tumour vessel normalization and potentiates anti-cancer therapies, Nat. Nanotechnol. 14 (12) (2019) 1160–1169.
[30] N. Endo, S. Oowada, Y. Sueishi, M. Shimmei, K. Makino, H. Fujii, Y. Kotake, Serum hydroxyl radical scavenging capacity as quantified with iron-free hydroxyl radical source, J. Clin. Biochem. Nutr. 45 (2) (2009) 193–201.
[31] S.J. Park, R.Y. Kim, B.W. Park, S. Lee, S.W. Choi, J.H. Park, J.J. Choi, S.W. Kim, J. Jang, D.W. Cho, H.M. Chung, S.H. Moon, K. Ban, H.J. Park, Dual stem cell therapy synergistically improves cardiac function and vascular regeneration following myocardial infarction, Nat. Commun. 10 (1) (2019) 3123.
[32] W. Cao, S. Peng, Y. Yao, J. Xie, S. Li, C. Tu, C. Gao, A nanofibrous membrane loaded with doxycycline and printed with conductive hydrogel strips promotes diabetic wound healing in vivo, Acta Biomater. 152 (2022) 60–73.
[33] Y. Zhao, D. Wang, T. Qian, J. Zhang, Z. Li, Q. Gong, X. Ren, Y. Zhao, Biomimetic nanozyme-decorated hydrogels with H_2O_2-activated oxygenation for modulating immune microenvironment in diabetic wound, ACS Nano 17 (17) (2023) 16854–16869.
[34] H. Chen, Y. Cheng, J. Tian, P. Yang, X. Zhang, Y. Chen, Y. Hu, J. Wu, Dissolved oxygen from microalgae-gel patch promotes chronic wound healing in diabetes, Sci. Adv. 6 (20) (2020) eaba4311.
[35] Q. Tang, Y. Tan, S. Leng, Q. Liu, L. Zhu, C. Wang, Cupric-polymeric nanoreactors integrate into copper metabolism to promote chronic diabetic wounds healing, Mater. Today Bio 26 (2024) 101087.
[36] T. Zhong, N. Gao, Y. Guan, Z. Liu, J. Guan, Co-delivery of bioengineered exosomes and oxygen for treating critical limb ischemia in diabetic mice, ACS Nano 17 (24) (2023) 25157–25174.
[37] A. Matsakas, V. Yadav, S. Lorca, R.M. Evans, V.A. Narkar, Revascularization of ischemic skeletal muscle by estrogen-related receptor-Γ, Circ. Res. 110 (8) (2012) 1087–1096.
[38] Q. Zhu, X. Liu, Q. Zhu, Z. Liu, C. Yang, H. Wu, L. Zhang, X. Xia, M. Wang, H. Hao, Y. Cui, G. Zhang, M.A. Hill, G.C. Flaker, S. Zhou, Z. Liu, N-acetylcysteine enhances the recovery of ischemic limb in type-2 diabetic mice, Antioxidants 11 (6) (2022) 1097.
[39] Y. Xu, M. Fu, Z. Li, Z. Fan, X. Li, Y. Liu, P.M. Anderson, X. Xie, Z. Liu, J. Guan, A prosurvival and proangiogenic stem cell delivery system to promote ischemic limb regeneration, Acta Biomater. 31 (2016) 99–113.
[40] Dilip Thomas, Arun Thirumaran, Beth Mallard, Xizhe Chen, Shane Browne, Antony M. Wheatley, Timothy O'Brien, Abhay Pandit, Variability in endogenous perfusion recovery of immunocompromised mouse models of limb ischemia, Tissue Eng. Part C Method. 22 (4) (2016) 370–381.
[41] Y.C. Sung, P.R. Jin, L.A. Chu, F.F. Hsu, M.R. Wang, C.C. Chang, S.J. Chiou, J.T. Qiu, D.Y. Gao, C.C. Lin, Y.S. Chen, Y.C. Hsu, J. Wang, F.N. Wang, P.L. Yu, A.S. Chiang, A.Y. Wu, J.J. Ko, C.P. Lai, T.T. Lu, Y. Chen, Delivery of nitric oxide with a nanocarrier promotes tumour vessel normalization and potentiates anti-cancer therapies, Nat. Nanotechnol. 14 (12) (2019) 1160–1169.
[42] H. Chen, Y. Guo, Z. Zhang, W. Mao, C. Shen, W. Xiong, Y. Yao, X. Zhao, Y. Hu, Z. Zou, J. Wu, Symbiotic algae-bacteria dressing for producing hydrogen to accelerate diabetic wound healing, Nano Lett. 22 (1) (2022) 229–237.
[43] I. Ohsawa, M. Ishikawa, K. Takahashi, M. Watanabe, K. Nishimaki, K. Yamagata, K. Katsura, Y. Katayama, S. Asoh, S. Ohta, Hydrogen acts as a therapeutic antioxidant by selectively reducing cytotoxic oxygen radicals, Nat. Med. 13 (6) (2007) 688–694.
[44] J. Yan, Z. Zhang, H. Shi, HIF-1 is involved in high glucose-induced paracellular permeability of brain endothelial cells, Cell. Mol. Life Sci. 69 (1) (2012) 115–128.
[45] H. Chen, Y. Cheng, J. Tian, P. Yang, X. Zhang, Y. Chen, Y. Hu, J. Wu, Dissolved oxygen from microalgae-gel patch promotes chronic wound healing in diabetes, Sci. Adv. 6 (20) (2020) eaba4311.
[46] S. Chen, Y. Zhu, Q. Xu, Q. Jiang, D. Chen, T. Chen, X. Xu, Z. Jin, Q. He, Photocatalytic glucose depletion and hydrogen generation for diabetic wound healing, Nat. Commun. 13 (1) (2022) 5684.
[47] P. Holden, L.S. Nair, Deferoxamine: an angiogenic and antioxidant molecule for tissue regeneration, Tissue Eng, Part B Rev. 25 (6) (2019) 461–470.
[48] S. Hu, Z. Li, D. Shen, D. Zhu, K. Huang, T. Su, P.U. Dinh, J. Cores, K. Cheng, Exosome-eluting stents for vascular healing after ischemic injury, Nat. Biomed. Eng. 5 (10) (2021) 1174–1188.
[49] T. Zhong, N. Gao, Y. Guan, Z. Liu, J. Guan, Co-delivery of bioengineered exosomes and oxygen for treating critical limb ischemia in diabetic mice, ACS Nano 17 (24) (2023) 25157–25174.
[50] E. Takematsu, M. Massidda, J. Auster, P.C. Chen, B.G. Im, S. Srinath, S. Canga, A. Singh, M. Majid, M. Sherman, A. Dunn, A. Graham, P. Martin, A.B. Baker, Transmembrane stem cell factor protein therapeutics enhance revascularization in ischemia without mast cell activation, Nat. Commun. 13 (1) (2022) 2497.
[51] H.S. Cheng, R.L. Zhuang, D. Pérez-Cremades, J.S. Chen, A. Jamaiyar, W. Wu, G. Sausen, A. Tzani, J. Plutzky, J. Henao-Mejia, P.P. Goodney, M.A. Creager, M. S. Sabatine, M.P. Bonaca, M.W. Feinberg, A miRNA/CXCR4 signaling axis impairs monopoiesis and angiogenesis in diabetic critical limb ischemia, JCI Insight 8 (7) (2023) e163360.